Journal of Sound and Vibration (1999) **224**(2), 283–303
Article No. jsvi.1999.2167, available online at http://www.idealibrary.com on IDEAL®

A GENERALIZED IMPEDANCE MATCHING METHOD FOR DETERMINING STRUCTURAL–ACOUSTIC POWER FLOW CONTROL LAWS

R. M. GLAESE* AND D. W. MILLER

Space Systems Laboratory, Space Engineering Research Center, Massachusetts Institute of Technology, Cambridge, Massachusetts 02139, *U.S.A.*

(*Received* 30 *January* 1998, *and in final form* 1 *February* 1999)

Impedance matching compensators are investigated for structural–acoustic control. The primary method for deriving these compensators is the minimization of acoustic power flow emanating from the structure–acoustic boundary. This work builds upon frequency domain wave control concepts. Unfortunately, due to the complexity of the solution, power flow minimization via Wiener filtering can only be used for extremely simple situations. Therefore, it is recast in a state space formulation that has a wealth of numerical tools, most notably the linear quadratic Gaussian (LQG) design technique. The equivalence between power flow minimization and the solution of the LQG problem is demonstrated on a simple one-dimensional structural–acoustic sample problem. To illustrate the LQG power flow derivation for more realistic systems, it is applied to a two-dimensional sample problem.

1. INTRODUCTION

Acoustic launch loads and their impact on payloads enclosed in aerodynamic fairings have begun to receive attention in the last several years [1–3]. Launch loads account for 40% of first day spacecraft failures. Reducing these loads gives the opportunity to use more off-the-shelf components, making the spacecraft cheaper and increasing the chance of mission success.

While payload isolation is a fairly well developed field, acoustic load alleviation has not received much attention. This is primarily due to the fact that the acoustic disturbances are weakly correlated with structural measurements, making adaptive feedforward schemes difficult. Feedback control is an alternative to feedforward control, but its performance is driven by the accuracy of a descriptive model of the structural–acoustic behavior. Fully coupled structural–acoustic models suffer from the sheer size required to achieve any fidelity in the model. Another disadvantage of the fully coupled model is that a

*Now with CSA Engineering, Inc.

0022–460X/99/270283 + 21 $30.00/0

different model must be formulated each time the payload geometry is changed. A locally coupled structural–acoustic model alleviates these disadvantages by not including a detailed model of the interior acoustics. The locally coupled model naturally leads to a particular control design technique: impedance matching.

Impedance matching has been used for purely structural systems for some time [4–6], but only recently has it been extended to structural–acoustic systems [7, 8]. In reference [8], Glaese *et al.* derive an impedance matching control law for a structural–acoustic system consisting of a one-dimensional acoustic waveguide connected to a single-degree-of-freedom structure. This impedance matching control law was compared to compensators designed using only a structural model and a fully coupled structural–acoustic model. For this simple academic example, it was shown that impedance matching achieved nearly 99% of the performance of a fully coupled model while satisfying all the imposed constraints on the control architecture: insensitivity to payload geometry and actuation/sensing that conforms to the structural geometry (i.e., no extra microphones or speakers in the acoustic field). The limitation of this result is that it is derived specifically for the one-dimensional case, where the acoustics can be simply described by leftward and rightward travelling waves. For more realistic situations, where the acoustics are three-dimensional and the structure is two-dimensional in nature, the impedance matching derivation is much more difficult, if not impossible. Moreover, the impedance matching design in reference [8] placed no limitations on control effort, possibly leading to difficulties in practical implementation. The results from reference [8], however, do indicate that the impedance matching approach does bridge the gap between the simplistic control design using only a structural model and the complex, expensive control design using a fully coupled structural–acoustic model. Thus, the purpose of this paper is to extend the impedance matching design in reference [8] to higher dimensional situations and to include penalties on the control effort.

The derivation of the impedance matching control law relies on the minimization of the power flow at the structure–acoustic boundary to determine the form of the compensator [4, 5]. This approach makes use of a local wave model of the structure–acoustic boundary in which the details of the acoustic field, namely the acoustic modes, are not necessary. This structural–acoustic wave model is equivalent to a state-space model of the structure with the acoustic pressure included as a disturbance affecting the structural dynamics. This structural model is much more readily available for realistic situations.

Since power flow can be written as a quadratic function of the travelling wave amplitudes, this suggests that an equivalency might be found between power flow minimization and a state-space control design technique, namely the linear quadratic Gaussian (LQG) technique, which requires several weighting matrices to determine the regulator and estimator gains. Thus, if the power flow emanating from the structure–acoustic boundary can be captured in these weighting matrices, LQG can be used to easily solve for the structural–acoustic impedance match in realistic situations. This equivalency will be demonstrated for a simple structural–acoustic system, shown in Figure 1.

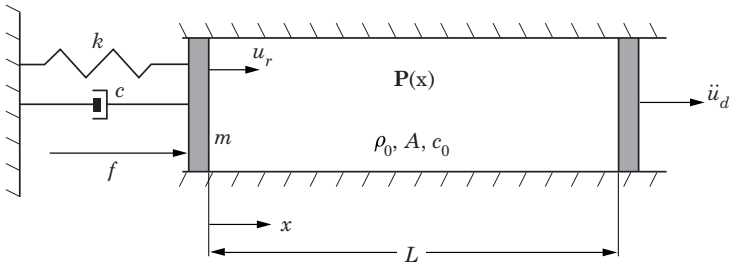

Figure 1. One-dimensional acoustic waveguide coupled with a one-degree-of-freedom structure.

This structural–acoustic system consists of a one-dimensional acoustic waveguide with a single-degree-of-freedom structure on the left end and disturbance source on the right end. The single-degree-of-freedom structure on the left end consists of a mass, spring, damper, and force, while the disturbance source is simply a massless piston that undergoes prescribed accelerations, $\ddot{u}_d$.

For this simple structural–acoustic system, the acoustics at any point in the waveguide obey the wave equation [9] given by

$$\partial^2 P/\partial x^2 - (1/c_0^2)\partial^2 P/\partial t^2 = 0, \tag{1}$$

where c_0 is the speed of sound. The structure, on the other hand, obeys the second order differential equation

$$m\ddot{u} + c\dot{u} + ku = f - AP, \tag{2}$$

where the acoustic pressure acts as a forcing term on the structural dynamics. At the structure–acoustic boundary, the relationship between acoustic pressure and structural motion is given by

$$\partial P/\partial x = -\rho_0 \ddot{u}, \tag{3}$$

where ρ_0 is the ambient density of the acoustic medium. The locally coupled structural–acoustic model is formed by ignoring the reverberant acoustics. Instead, only the force on the structure caused by the acoustic pressure and the influence of structural motion on the acoustic field are included since they are sufficient to capture the mechanisms which govern how power is transferred from the acoustic medium to the structure and vice versa. This first effect is seen in the second term on the right side of equation (2), while the second effect is seen in equation (3). This system will now be used to derive impedance matching compensators using power flow minimization and LQG.

2. POWER FLOW MINIMIZATION

Average acoustic power per unit area radiated at a structure–acoustic boundary can be written in a quadratic form given by reference [9]

$$\mathcal{P} = \frac{1}{T}\int_0^T P(t)\dot{u}(t)\,\mathrm{d}t, \tag{4}$$

where $P(t)$ is the acoustic pressure, and $\dot{u}(t)$ is the acoustic particle velocity (also the structural velocity). If one considers a vibrating piston with area, A, the average acoustic power flow becomes

$$\mathcal{P} = \frac{1}{T}\int_0^T P(t)A\dot{u}(t)\,\mathrm{d}t. \tag{5}$$

Using the relationship between $\dot{u}(t)$ and the pressure gradient, $\partial P/\partial x$, this average power flow can be written in terms of the so-called acoustic state variables P and $\partial P/\partial x$. Furthermore, if one uses the Power Theorem, a variation of Parseval's Theorem, one can write the average power flow in the frequency domain as

$$\mathcal{P} = \frac{1}{2\pi}\int_{-\infty}^{+\infty} AP(\omega)\dot{u}(\omega)\,\mathrm{d}\omega = \frac{1}{2\pi}\int_{-\infty}^{+\infty} P(\omega)A\left(-\frac{1}{j\omega\rho_0}\frac{\partial P(\omega)}{\partial x}\right)\mathrm{d}\omega. \tag{6}$$

We can now introduce leftward and rightward traveling waves, such that

$$P(x, t) = P_l\,\mathrm{e}^{\mathrm{i}\hat{k}x+\mathrm{i}\omega t} + P_r\,\mathrm{e}^{-\mathrm{i}\hat{k}x+\mathrm{i}\omega t}, \tag{7}$$

where $\hat{k}$ is the wave number, which can be thought of as a spatial frequency, and is also related to temporal frequency through the dispersion relation

$$\hat{k} = \omega/c_0. \tag{8}$$

The acoustic state variables, then, are related to the wave amplitudes through the matrix equation

$$\begin{bmatrix} P \\ \partial P/\partial x \end{bmatrix} = \begin{bmatrix} 1 & 1 \\ \mathrm{i}\hat{k} & -\mathrm{i}\hat{k} \end{bmatrix}\begin{bmatrix} P_l \\ P_r \end{bmatrix}. \tag{9}$$

Using these relations, one can show [5] that the power flow has the form

$$\mathcal{P}(\omega) = \tfrac{1}{2}[w_i(\omega)^{\mathrm{H}} w_o(\omega)^{\mathrm{H}}]\mathcal{P}_m\begin{bmatrix} w_i(\omega) \\ w_o(\omega) \end{bmatrix}. \tag{10}$$

In order to avoid confusion with the structure–acoustic boundary power flow matrix, $\mathcal{P}_m$, the incoming and outgoing pressure wave amplitudes relative to the structure–acoustic boundary are denoted by w_i and w_o, respectively. The power flow matrix for the acoustic case is given by (incoming power is defined to be negative)

$$\mathcal{P}_m = \begin{bmatrix} \mathcal{P}_{ii} & \mathcal{P}_{io} \\ \mathcal{P}_{oi} & \mathcal{P}_{oo} \end{bmatrix} = \frac{2}{\rho_0 c_0}\begin{bmatrix} -A & 0 \\ 0 & A \end{bmatrix}. \tag{11}$$

The incoming acoustic waves are thought of as a disturbance to the structure. In order to reduce (or eliminate) the power of the outgoing waves, this disturbance is measured and fed to the structural actuator in a feedforward scheme. This scheme is shown in Figure 2 where $F(\omega)$ is the feedforward compensator and P_o is related to P_i and the actuator force Q by the scattering matrix, $\mathbf{S}(\omega)$, and the generation matrix, $\mathbf{\Psi}(\omega)$, as in

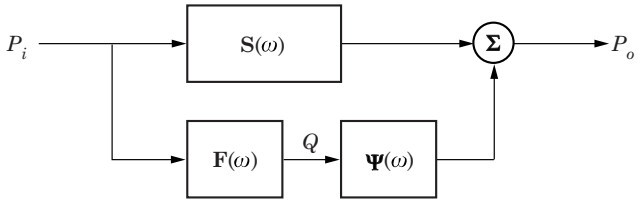

Figure 2. Feedforward of incoming wave modes.

$$P_o(\omega) = \mathbf{S}(\omega)P_i(\omega) + \mathbf{\Psi}(\omega)Q(\omega). \tag{12}$$

The models of the structure and control input are captured in $\mathbf{S}(\omega)$ and $\mathbf{\Psi}(\omega)$.

Unfortunately, the wave amplitudes are usually impossible to measure in reality. Therefore, the control must be formulated using physically measurable quantities, such as pressure and acceleration. Figure 3 shows a feedback scheme block diagram which uses physical measurements, u. The compensator in this scheme is denoted by G. The terms Y_{ui} and Y_{uo} relate the physical measurements to the incoming and outgoing wave amplitudes, respectively.

The block diagram of Figure 3 can be rearranged to put it in a form similar to that of Figure 2. This rearranged block diagram is shown in Figure 4 and illustrates the disturbance rejection problem where incoming waves are rejected by feeding back physical measurements to the physical actuators.

The optimization problem becomes the minimization of the expected steady state power flow plus control effort. Summing over all frequencies gives the total power flow when the system is undergoing steady state motion. Adding a quadratic control effort penalty to the power term in equation (10) and taking the expected value of the resulting integral expression gives a scalar cost functional,

$$\begin{aligned} J &= \tfrac{1}{2}E\left\{\int_{-\infty}^{+\infty} (w^{\mathrm{H}}\mathcal{P}_m w + f^{\mathrm{H}}\rho f)\, \mathrm{d}\omega\right\} \\ &= \tfrac{1}{2}\int_{-\infty}^{+\infty} \mathrm{trace}\{E(\mathcal{P}_m w w^{\mathrm{H}} + \rho f f^{\mathrm{H}})\}\, \mathrm{d}\omega, \end{aligned} \tag{13}$$

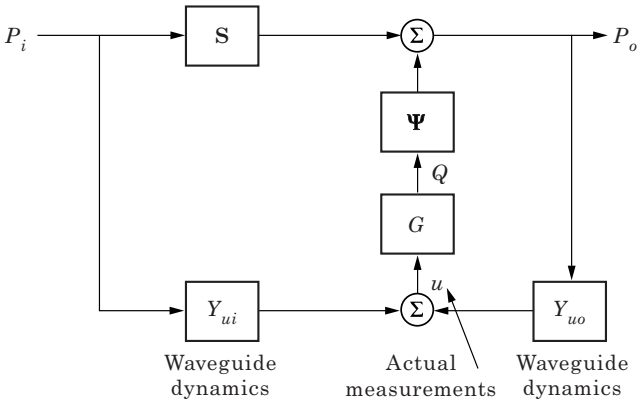

Figure 3. Feedback of physical measurements.

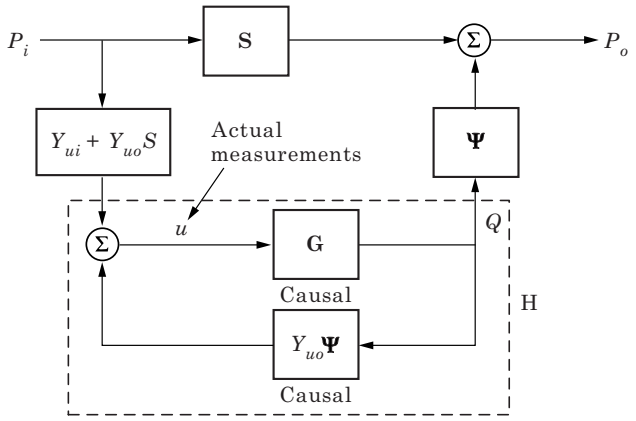

Figure 4. Physical measurement feedback to mimic feedforward of incoming wave modes.

where ρ is the control penalty, not to be confused with the ambient density ρ_0. It is assumed in the optimization that the only available feedback sensor is the pressure at the structure–acoustic boundary, P. The optimization, then, is to find a compensator $G(s)$ that minimizes equation (13) with

$$f = G(s)P. \tag{14}$$

Up to this point, the derivation has been rather generic, equally applicable to structural or acoustic systems. For the sake of brevity, however, the rest of the derivation will be specialized for the system shown in Figure 1. Further details on the minimization of the cost in equation (13) can be found in Miller *et al.* [5] It can be shown (reference [8]) that at the structure–acoustic boundary the outgoing reflected wave amplitude is related to the incoming wave amplitude and the forcing on the structure by

$$w_o = \frac{ms^2 + (c - \rho_0 c_0 A)s + k}{ms^2 + (c + \rho_0 c_0 A)s + k} w_i + \frac{\rho_0 c_0 s}{ms^2 + (c + \rho_0 c_0 A)s + k} f. \tag{15}$$

Using the relations in equation (15) to minimize the cost, J, results in a compensator transfer function,

$$G_\rho(s) = \frac{s(ms^2 + (c - \rho_0 c_0 A)s + k)}{\text{den}}, \tag{16}$$

where

$$\text{den} = m^2\rho s^4 - m\rho\rho_0 c_0 A s^3 + (2km\rho - c\rho(c + \rho_0 c_0 A) - \rho_0 c_0)s^2$$
$$- k\rho\rho_0 c_0 A s + k^2\rho. \tag{17}$$

There are several things to note about this transfer function. First, if $\rho = 0$, then the impedance matching result from reference [8] is recovered (see below):

$$G(s) = -(ms^2 + (c - \rho_0 c_0 A)s + k)/\rho_0 c_0 s. \tag{18}$$

The main difference between the compensators in equations (16) and (18) is the presence of a control penalty, ρ. Unfortunately, the presence of the control penalty makes the denominator have roots in the right half of the complex Laplace plane. Because the system is open-loop stable, the feedforward compensator must also be stable for the closed-loop system to be stable. Since the compensator is stable and there are right half plane poles in the compensator, $G_\rho(s)$ is non-causal and requires information from future time. The net result of the non-causality is that this compensator cannot be implemented in practice and a constraint on the causality of the impedance matching compensator must be imposed in the power flow minimization.

The causal compensator which minimizes the cost in equation (13) can be found by Wiener–Hopf techniques, which is discussed in more detail in Miller *et al*. [5] Once again for the sake of brevity, since the solution is quite involved, only the resulting causal compensator will be presented here. This compensator, $G_{\rho,causal}(s)$, is given by the expression

$$G_{\rho,causal}(s) = g_2(s)(ms^2 + (c + \rho_0 c_0 A)s + k)/(2\sqrt{\rho}\omega_c g_1(s) - \rho_0 c_0 s g_2(s)), \tag{19}$$

where

$$g_1(s) = (s + \sqrt{C_1})(s + \sqrt{C_2})(ms^2 + cs + k), \tag{20}$$

$$g_2(s) = C_3(s - p_1)(s - p_2) + C_4(s + \omega_c)(s - p_2) + C_5(s + \omega_c)(s - p_1), \tag{21}$$

$$p_{1,2} = -(c + \rho_0 c_0 A)/2m \pm \sqrt{([c + \rho_0 c_0 A]/2m)^2 - k/m}, \tag{22}$$

$$C_{1,2} = (-k/m + \tfrac{1}{2}([c + \rho_0 c_0 A]/m)^2 + \rho_0 c_0/m^2\rho) \pm \sqrt{(k/m - \tfrac{1}{2}([c + \rho_0 c_0 A]/m)^2 - \rho_0 c_0/m^2\rho)^2 - k^2/m^2}, \tag{23}$$

$$C_3 = \frac{2\omega_c^2(\omega_c^2 - [(c - \rho_0 c_0 A)/m]\omega_c + k/m)}{m\sqrt{\rho}(\omega_c + \sqrt{C_1})(\omega_c + \sqrt{C_2})(\omega_c + p_1)(\omega_c + p_2)}, \tag{24}$$

$$C_4 = \frac{-2\omega_c p_1(p_1^2 - [(c - \rho_0 c_0 A)/m]p_1 + k/m)}{m\sqrt{\rho}(p_1 - \sqrt{C_1})(p_1 - \sqrt{C_2})(p_1 - p_2)(p_1 + \omega_c)}, \tag{25}$$

$$C_5 = \frac{-2\omega_c p_2(p_2^2 - [(c - \rho_0 c_0 A)/m]p_2 + k/m)}{m\sqrt{\rho}(p_2 - \sqrt{C_1})(p_2 - \sqrt{C_2})(p_2 - p_1)(p_2 + \omega_c)}. \tag{26}$$

The ω_c in these expressions comes from a frequency weighting on the incoming wave amplitude. This frequency weighting takes the form of a unity-gain low-pass filter,

$$G_f(s) = \omega_c/(s + \omega_c). \tag{27}$$

The weighting serves two purposes, the first of which is to emphasize the power flow below a cut-off frequency, ω_c. The second reason for this weighting is that it is necessary for proper conditioning of the LQG problem, which will be explained shortly.

As expected, the compensator of equation (19) has only left half plane poles and hence, is causal, making it possible to implement this compensator. Although it appears rather complicated, the frequency response of this compensator is actually rather similar to those of equations (16) and (18), as might be expected, since they both minimize the same cost.

In the formulation of the power flow minimization it was implicitly assumed that the incoming waves are uncorrelated with the outgoing waves. Clearly, since the structural–acoustic system is finite in extent, the outgoing waves will eventually reflect from the acoustic boundary at the other end to return as incoming waves, making this assumption invalid. Furthermore, there is no guarantee that power will be dissipated by the compensator. In fact, the compensator may amplify power in some frequency range to minimize it in another. As far as the local compensator is concerned, this is not a problem, but for a finite system, the combination of the return of outgoing power and power amplification can lead to instability for the fully reverberant system.

Several approaches can be used to address the possibility of instability [5, 10]. The first approach [5] involves an iterative process where the causal compensator is computed and the resulting closed-loop power flow computed. If the closed-loop power flow is positive (amplification) in any frequency range, the design parameters are adjusted and the compensator recomputed. In the second approach [10], the solution procedure may be constrained such that the closed-loop power flow is less than or equal to zero for all frequencies. The final approach involves trying to correlate the incoming waves with the outgoing waves. This approach, however, requires information about the entire system, which is to be avoided. The simplest of these, and the one used in this paper, is the iterative approach, in which the control penalty is changed in response to positive power flow in any frequency range.

The complexity of the solution for this very simple sample problem is proof enough that a better method for obtaining the causal impedance matching compensator with finite control penalty is needed. Thus, this power flow approach and solution provides motivation for the use of a simpler and more automated method for deriving the compensator. This simpler method is found in the LQG design technique using a state space structural model with local acoustic coupling.

3. LQG IMPEDANCE MATCHING DESIGN

The linear quadratic Gaussian (LQG) design technique is a well known design technique consisting of two parts, the regulator and the estimator. LQG determines a compensator, with regulator gains **G** and estimator gains **H**, of the form

$$\dot{\hat{x}}(t) = (\mathbf{A} - \mathbf{BG} - \mathbf{HC}_y + \mathbf{BD}_{yu}\mathbf{C}_y)\hat{x}(t) + \mathbf{H}y(t), \quad u(t) = -\mathbf{G}\hat{x}(t), \tag{28, 29}$$

which minimizes the quadratic cost given by

$$J_{LQG} = \tfrac{1}{2}E\left\{\int_{-\infty}^{+\infty} (x^{\mathrm{H}}\mathbf{C}_z^T\mathbf{Q}\mathbf{C}_z x + u^{\mathrm{H}}\rho u)\, \mathrm{d}\omega\right\}, \tag{30}$$

subject to the constraints

$$\dot{x}(t) = \mathbf{A}x(t) + \mathbf{B}u(t) + \mathbf{L}\xi(t), \quad y(t) = \mathbf{C}_y x(t) + \mathbf{D}_{yu}u(t) + \eta(t), \quad z(t) = \mathbf{C}_z x(t), \tag{31–33}$$

where ξ and η are Gaussian white noises representing process noise and sensor noise, respectively. The vector y represents the sensor measurements, while z represents the performance variables.

Comparison of equation (30) with the power flow cost of equation (13) reveals that they are nearly identical. The only difference between the two is the choice of state variables and the difference in weighting matrices, $\mathcal{P}_m$ versus $\mathbf{Q}$. Thus, it becomes clear that if the state variables in the power flow case can be related to the performance variables in the state-space system and $\mathbf{Q}$ can be related to the power matrix, $\mathcal{P}_m$, then LQG may arrive at the same solution as the power flow minimization.

Since LQG is a state-space technique, the structural equation of motion in equation (2) must be put in second order form:

$$\begin{bmatrix} \dot{u} \\ \ddot{u} \end{bmatrix} = \begin{bmatrix} 0 & 1 \\ -k/m & -c/m \end{bmatrix} \begin{bmatrix} u \\ \dot{u} \end{bmatrix} + \begin{bmatrix} 0 & 0 \\ 1/m & -A/m \end{bmatrix} \begin{bmatrix} f \\ P \end{bmatrix}. \tag{34}$$

The total surface acoustic pressure is shown as a disturbance in the state-space system. However, a portion of this pressure is created by the motion of the structure and is therefore correlated with its dynamics. In order to have an uncorrelated disturbance, the more natural disturbance is the pressure associated with an incoming acoustic wave. It then follows that the most natural performance variable is a combination of the incoming and outgoing acoustic pressure waves, i.e. the power. The natural feedback sensor measurement is total surface acoustic pressure, because it can be physically measured. Fortunately, relations between the total surface acoustic pressure and the incoming and outgoing pressure wave amplitudes can be determined from equations (3) and (9). These relations are

$$w_o = w_i + \rho_0 c_0 \dot{u}; \quad P = 2w_i + \rho_0 c_0 \dot{u}. \tag{35, 36}$$

This results in the following state-space system

$$\begin{bmatrix} \dot{u} \\ \ddot{u} \end{bmatrix} = \begin{bmatrix} 0 & 1 \\ -k/m & -(c + \rho_0 c_0 A)/m \end{bmatrix} \begin{bmatrix} u \\ \dot{u} \end{bmatrix} + \begin{bmatrix} 0 & 0 \\ 1/m & -2A/m \end{bmatrix} \begin{bmatrix} f \\ w_i \end{bmatrix}, \tag{37}$$

$$y = P = [0 \quad \rho_0 c_0] \begin{bmatrix} u \\ \dot{u} \end{bmatrix} + 2w_i, \quad z = \begin{bmatrix} w_i \\ w_0 \end{bmatrix} = \begin{bmatrix} 0 & 0 \\ 0 & \rho_0 c_0 \end{bmatrix} \begin{bmatrix} u \\ \dot{u} \end{bmatrix} + \begin{bmatrix} 1 \\ 1 \end{bmatrix} w_i. \quad (38, 39)$$

The fact that there is a feedthrough term from the disturbance w_i in the performance equation (39) implies that there is infinite energy in the disturbance to performance transfer function and cannot be altered by the control. In order to avoid this situation, a unity gain low pass filter can be added to the disturbance input, which results in the state-space equations

$$\begin{bmatrix} \dot{u} \\ \ddot{u} \\ \dot{w}_i \end{bmatrix} = \begin{bmatrix} 0 & 1 & 0 \\ -k/m & -(c + \rho_0 c_0 A)/m & -2A/m \\ 0 & 0 & -\omega_c \end{bmatrix} \begin{bmatrix} u \\ \dot{u} \\ w_i \end{bmatrix} + \begin{bmatrix} 0 \\ 1/m \\ 0 \end{bmatrix} f + \begin{bmatrix} 0 \\ 0 \\ \omega_c \end{bmatrix} \xi, \quad (40)$$

$$y = P = [0 \quad \rho_0 c_0 \quad 2] \begin{bmatrix} u \\ \dot{u} \\ w_i \end{bmatrix}, \quad z = \begin{bmatrix} w_i \\ w_o \end{bmatrix} = \begin{bmatrix} 0 & 0 & 1 \\ 0 & \rho_0 c_0 & 1 \end{bmatrix} \begin{bmatrix} u \\ \dot{u} \\ w_i \end{bmatrix}. \quad (41, 42)$$

This set of state-space equations are the final set from which an LQG compensator is determined. Power flow minimization does not make provisions for sensor noise but LQG does. In order to maintain consistency between the two solution methods, the estimator gains for LQG must be determined using a sensor noise intensity approaching zero. The sensor noise cannot be exactly zero due to constraints on the Riccati equation. The last step is to determine the weighting matrix $\mathbf{Q}$. Since the performance variables are the incoming and outgoing pressure wave amplitudes, the obvious choice for $\mathbf{Q}$ is simply the entire $\mathcal{P}_m$ matrix. In order to guarantee a positive definite solution to the regulator Riccati equation, though, $\mathbf{Q}$ should be positive semi-definite, which is not the case for $\mathcal{P}_m$. This does not mean, however, that there is no solution to the Riccati equation. It is a reasonable assumption that there will be a solution to the Riccati equation since the direct power flow minimization found a solution. Alternatively, the performance could just include outgoing power which does provide a positive semi-definite $\mathbf{Q}$.

The assumption that the outgoing and incoming waves are uncorrelated has also been made for the LQG case. In a similar manner as the power flow minimization, an iterative procedure is implemented using LQG, in which the closed-loop power flow is computed. If the power flow is positive at any point, the design parameters are adjusted and the compensator rederived.

The LQG regulator and estimator gains $\mathbf{G}$ and $\mathbf{H}$ are derived from two uncoupled algebraic Riccati equations. Due to the low order of the system under consideration, it might be tempting to try to analytically solve the two Riccati equations. Unfortunately, even this very small system leads to algebraic expressions that cannot be analytically solved. Thus, the only remaining option is to evaluate the LQG compensators numerically.

4. POWER FLOW–LQG EQUIVALENCE

In order to compare the power flow and LQG compensators, the system parameters of Figure 1 must be given numerical values. The single-degree-of-freedom "structure" is sized to give a modal frequency of 37 Hz with 1% damping ($m = 0{\cdot}727$ kg, $k = 3{\cdot}93 \times 10^4$ N/m^2, $c = 3{\cdot}38$ Ns/m). The acoustic waveguide is then sized to give a fundamental acoustic frequency of 56 Hz ($\rho_0 = 1{\cdot}2$ kg/m^3, $c_0 = 346$ m/s, $A = 0{\cdot}0491$ m^2, $L = 3{\cdot}09$ m). These values are sized such that the fundamental structural and acoustic frequencies match those of a typical payload fairing.

Using these parameter values, the power flow and LQG compensator frequency responses can be computed for a given control penalty, ρ. Figure 5 shows the frequency response of the causal power flow compensator of equation (19) for different values of ρ. Figure 6 shows the frequency response of the LQG compensator (with nearly zero sensor noise) for the same values of ρ as in Figure 5. In both plots, the compensator magnitude increases as the control penalty decreases. Also, the dashed line in both plots is the frequency response of the unconstrained power flow compensator with zero control penalty, given by equation (18). Note in both cases that as the control penalty is decreased toward zero, the compensator frequency responses approach the unconstrained power flow compensator of equation (18). This is to be expected from the power flow compensator. For the LQG compensator, however, this fact provides evidence that the LQG formulation of the previous section is indeed the proper one to use to derive an implementable impedance matching compensator.

Careful comparison of the power flow frequency response with the LQG frequency response reveals that for a given value of ρ, they are identical. This shows that with the proper system formulation and weighting matrices, LQG returns the same compensator as power flow minimization with the causality

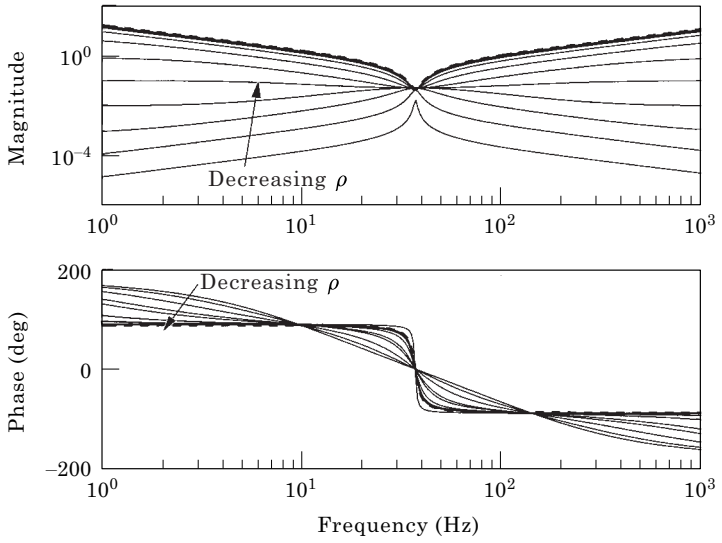

Figure 5. Causally constrained power flow minimization compensator frequency response for decreasing values of ρ.

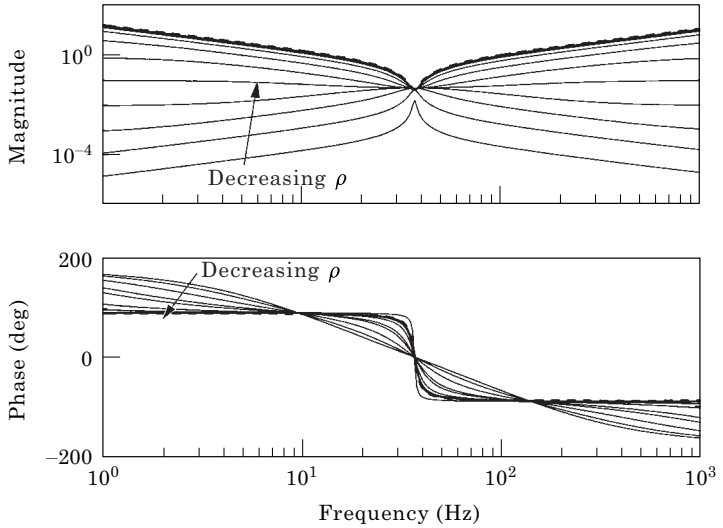

Figure 6. LQG compensator frequency response for decreasing values of ρ.

constraint. While this example is rather academic, the impact of this result on realistic systems is enormous. An impedance matching compensator can be derived from a model of an enclosing structure and its local acoustic coupling.

Closed-loop stability of a control system is always an important issue, especially in this case, where the design model and truth model are not identical. As mentioned previously, the power flow at the structural–acoustic boundary can be used to evaluate stability. If the power flow is negative at all frequencies,

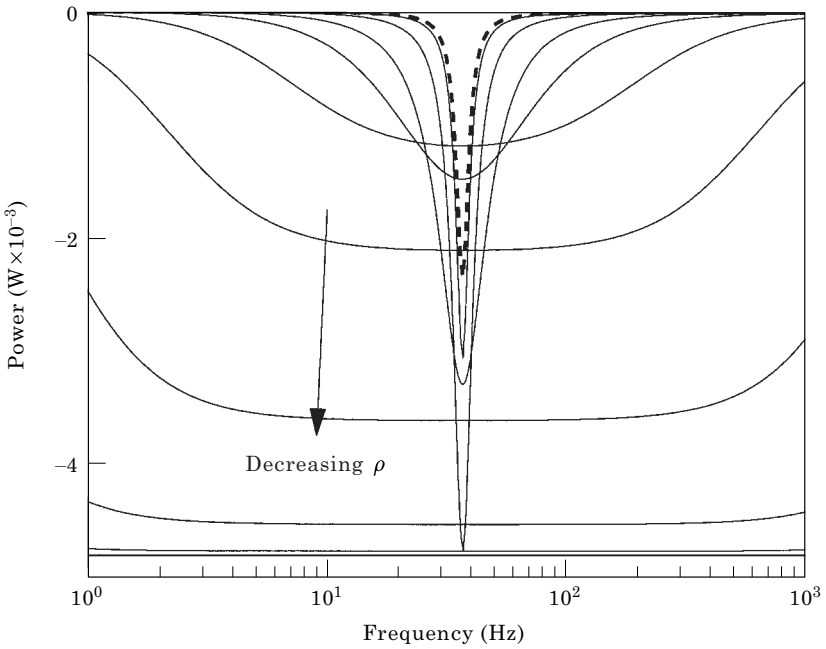

Figure 7. Open- (- - -) and closed-loop (—) power flow for LQG compensators.

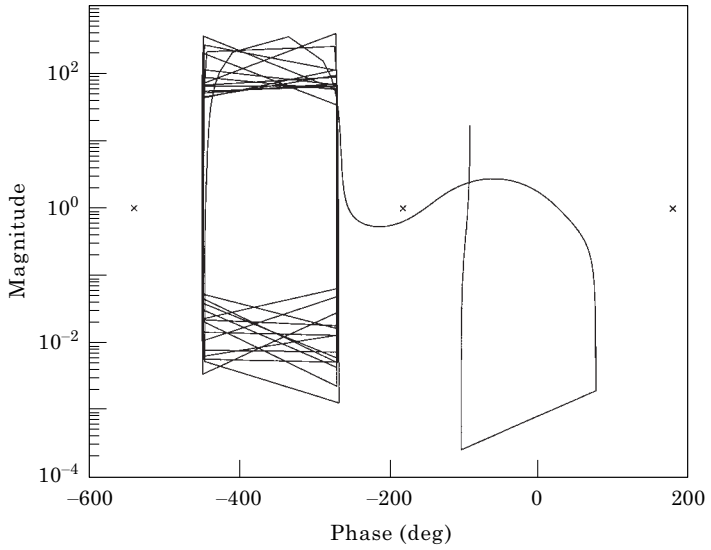

Figure 8. Nichols chart for stability of LQG power flow compensators.

indicating power dissipation, the fully reverberant closed-loop system will be stable. Figure 7 shows the power flow transfer functions for the compensators in Figures 5 and 6. Note that the open-loop power flow, dashed line, is always less than or equal to zero, indicating open-loop stability. The large dip at 37 Hz in the open-loop power flow transfer function is due to the dissipation in the structural dashpot. Note that all closed-loop power flow transfer functions are also less than or equal to zero, again indicating stability of the fully reverberant system. Since the power flow compensator is single input, single output (SISO), standard frequency domain techniques can also be used to evaluate stability of the reverberant system. Figure 8 shows the Nichols chart for one of the LQG compensators evaluated on the fully reverberant model. Note that there are no encirclements of the critical points, denoted by "x", and the reverberant closed-loop system is stable.

5. EXTENSION TO HIGHER DIMENSIONS

To illustrate the LQG power flow compensator design on a more realistic (i.e., higher dimensional) system, the sample problem in Figure 9 is considered. This sample problem consists of a two-dimensional acoustic cavity with a flexible wall on the left side that behaves like a simply supported Bernoulli–Euler beam. In the bottom right corner of the cavity is a disturbance source much the same as in the one-dimensional case. The parameters of the system are again set such that the fundamental structural mode is 37 Hz and the fundamental acoustic mode is 56 Hz. This sample problem, while fairly simple, actually captures all the essential features of real structural–acoustic systems, namely a multi-dimensional acoustic field, a structure with distributed mass and stiffness, and the possibility of distributed actuation and sensing.

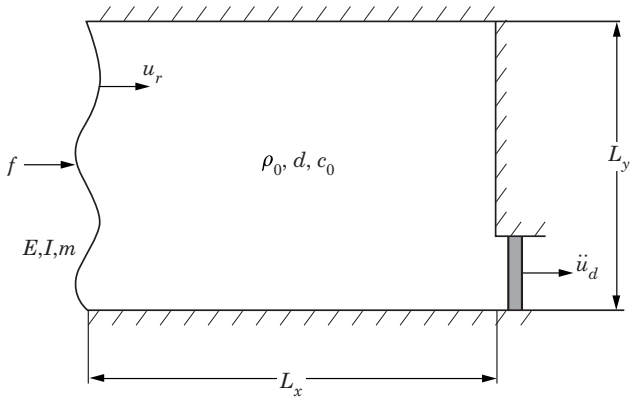

Figure 9. Two-dimensional acoustic cavity with a flexible wall.

The finite element method is used to model the beam and as such there are two degrees of freedom at each nodal point, displacement and its spatial derivative: rotation. A finite element model is chosen because this is the most likely structural model available for designing a power flow compensator in a realistic situation. The available actuators for the beam are forces and moments at each beam degree of freedom.

The structural finite element model consists of mass, stiffness, and damping matrices, $\mathbf{M}_s$, $\mathbf{K}_s$, and $\mathbf{C}_{ds}$. A modal model is also a possibility, but is not considered here. While damping matrices are not typically part of the finite element formulation, an *ad hoc* damping matrix may be determined from the structural mode shapes and the modal damping ratios. Along with the finite element matrices is the actuation matrix, $\mathbf{B}$, containing the influence of the forcing terms on the structure. To complete the necessary elements for the LQG formulation the local coupling between the structure and the acoustic field must be determined. This may also be performed using the finite element method by assuming shape functions in terms of nodal acoustic variables [11]. This results in a matrix, $\mathbf{A}_{fs}$, which describes the influence of the acoustic field on the structure, much the same as the actuation matrix, $\mathbf{B}$. The matrix $\mathbf{A}_{fs}$ can be thought of as a generalized area matrix, containing the nodal area for each structural element. This results in a state space system of the form

$$\begin{bmatrix} \dot{\vec{u}} \\ \ddot{\vec{u}} \end{bmatrix} = \begin{bmatrix} 0 & \mathbf{I} \\ -\mathbf{M}_s^{-1}\mathbf{K}_s & -\mathbf{M}_s^{-1}\mathbf{C}_{ds} \end{bmatrix} \begin{bmatrix} \vec{u} \\ \dot{\vec{u}} \end{bmatrix} + \begin{bmatrix} 0 & 0 \\ \mathbf{M}_s^{-1}\mathbf{B} & -\mathbf{M}_s^{-1}\mathbf{A}_{fs} \end{bmatrix} \begin{bmatrix} \vec{f} \\ \vec{P} \end{bmatrix}, \tag{43}$$

where $\vec{u}$ is the vector of structural displacements, $\vec{f}$ is the vector of structural forcing terms, and $\vec{P}$ is the vector of surface acoustic variables.

The simplest acoustic finite element formulation uses only the pressure at each nodal point. In this case there is a mismatch between the number of structural nodal degrees of freedom (2) and the number of acoustic nodal degrees of freedom (1). It can be argued that the missing acoustic variable is the pressure gradient tangential to the surface of the structure. It is intuitively obvious from the simple one-dimensional problem that pressure is analogous to structural

displacement. Therefore, since the extra structural degree of freedom is the spatial derivative of displacement along the axis of the beam, it seems reasonable to assume that the missing acoustic variable must also be a derivative along the beam axis, i.e., the tangential acoustic pressure gradient.

Several options are available to resolve this discrepancy. The first is to simply ignore the mismatch in both the structural–acoustic coupling and incoming/outgoing acoustics, using only pressure variables in formulating the LQG problem. The second option is to again ignore the missing acoustic variable in the structural–acoustic coupling, but to approximate it in the incoming/outgoing acoustics, using the acoustic element shape functions to find the missing acoustic variables. The final option is to augment the acoustic nodal degrees of freedom with the missing variable, hence including it in both the structural–acoustic coupling and incoming/outgoing acoustics. However, because this extra degree of freedom is needed only for the local model, it need not be included in a global model used for control evaluation. The last method is used here because it contains the most information about the acoustic field. Consequently, controllers designed using this model attain the highest performance.

The rest of the LQG formulation proceeds exactly the same as for the one-dimensional case. The total surface acoustic variables and outgoing acoustic variables are related to the incoming acoustic variables through

$$\vec{P}_o = \vec{P}_i + \rho_0 c_0 \dot{\vec{u}}, \quad \vec{P} = 2\vec{P}_i + \rho_0 c_0 \dot{\vec{u}}. \tag{44, 45}$$

Once again low-pass shaping filters must be added to the incoming acoustic disturbance, resulting in the following state space system, which may be used in LQG with low noise sensors.

$$\begin{bmatrix} \dot{\vec{u}} \\ \ddot{\vec{u}} \\ \dot{\vec{P}} \end{bmatrix} = \mathbf{A}_{local} \begin{bmatrix} \vec{u} \\ \dot{\vec{u}} \\ \vec{P}_i \end{bmatrix} + \begin{bmatrix} 0 \\ \mathbf{M}_s^{-1}\mathbf{B} \\ 0 \end{bmatrix} \vec{f} + \begin{bmatrix} 0 \\ 0 \\ \omega_c \mathbf{I} \end{bmatrix} \vec{\omega}, \tag{46}$$

$$\mathbf{A}_{local} = \begin{bmatrix} 0 & \mathbf{I} & 0 \\ -\mathbf{M}_s^{-1}\mathbf{K}_s & -\mathbf{M}_s^{-1}\mathbf{C}_{dfs} & -2\mathbf{M}_s^{-1}\mathbf{A}_{fs} \\ 0 & 0 & -\omega_c \mathbf{I} \end{bmatrix}, \quad \vec{y} = \vec{P} = [0 \quad \rho_0 c_0 \mathbf{I} \quad 2\mathbf{I}] \begin{bmatrix} \vec{u} \\ \dot{\vec{u}} \\ \vec{P}_i \end{bmatrix}, \tag{47, 48}$$

$$\vec{z} = \begin{bmatrix} \vec{P}_i \\ \vec{P}_o \end{bmatrix} = \begin{bmatrix} 0 & 0 & \mathbf{I} \\ 0 & \rho_0 c_0 I & \mathbf{I} \end{bmatrix} \begin{bmatrix} \vec{u} \\ \dot{\vec{u}} \\ \vec{P}_i \end{bmatrix}, \quad \mathbf{Q} = \frac{2}{\rho_0 c_0} \begin{bmatrix} -\mathbf{A}_{fs} & 0 \\ 0 & \mathbf{A}_{fs} \end{bmatrix}. \tag{49, 50}$$

For comparative purposes, Figure 10 shows a contour plot of the open-loop r.m.s. pressure map. The pressures shown in Figures 10 and 11 are those that arise due to a white noise disturbance emanating from the bottom right corner of the acoustic cavity. Figure 11 shows a similar contour plot for the closed-loop r.m.s. pressure map for a LQG power flow compensator with full actuation, meaning that each structural degree of freedom has an associated actuator. Note that the closed-loop pressure is much smaller than in open-loop example,

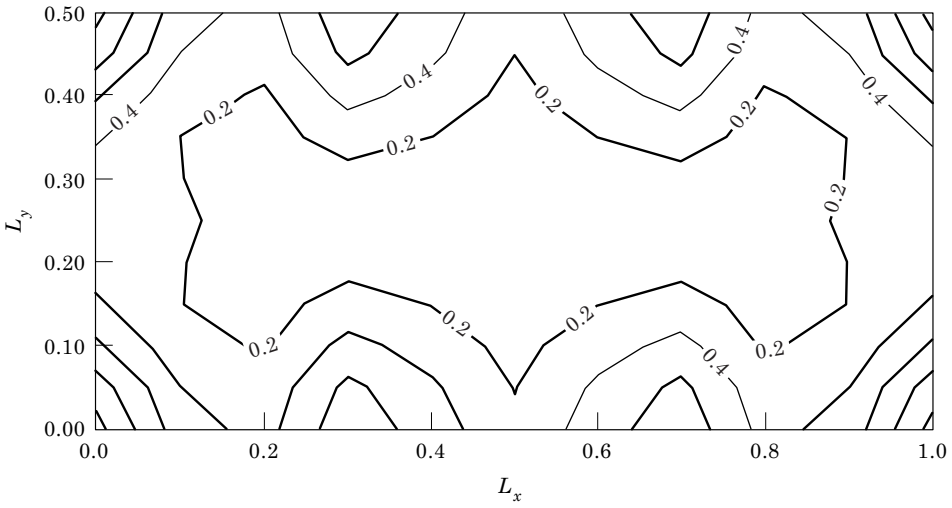

Figure 10. Contour plot of open-loop r.m.s. pressure map.

decaying smoothly from the disturbance source on the right side to the flexible wall on the left side. This feature is typical of power flow compensators, which cause the structure to interact with the acoustics as if it were an infinite cavity of fluid. This effect essentially destroys all modal behavior in the cavity. If acoustic modes were still present, they would show up in the pressure map as several localized peaks or hotspots. Because the beam has full actuation, the compensator is able to achieve an essentially perfect impedance match of the acoustics.

Figure 12 shows the open- and closed-loop power flow transfer functions at the flexible wall for the two-dimensional sample problem. Since incoming power

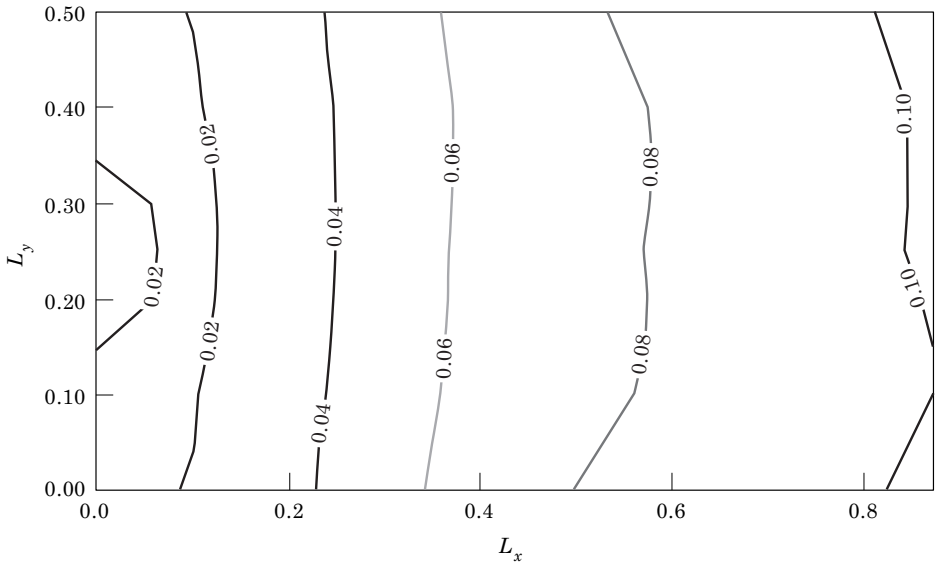

Figure 11. Contour plot of closed-loop r.m.s. pressure map for full actuation case.

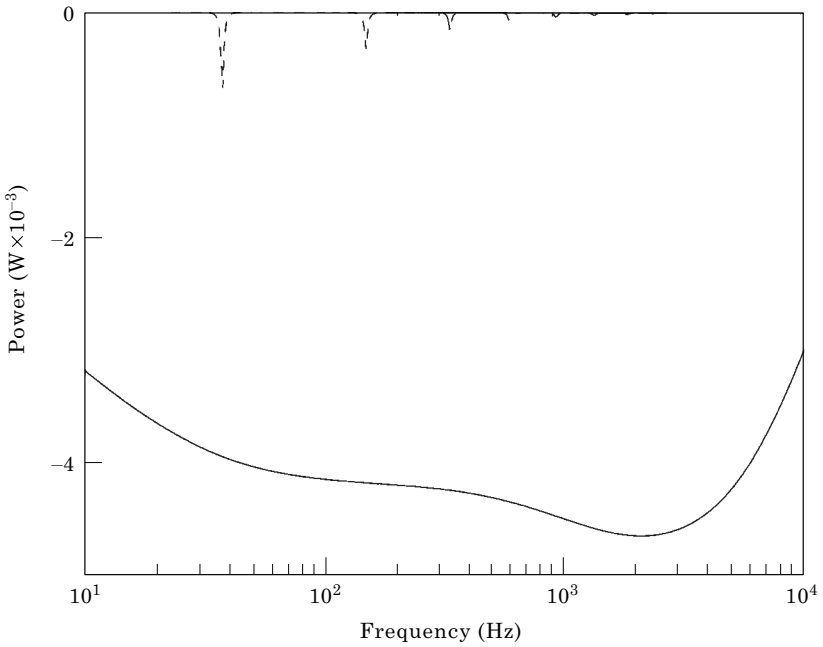

Figure 12. Open (- - -) and closed-loop (—) power flow transfer functions for full actuation case.

is defined as negative, negative power flow indicates that more power is incoming than outgoing at a particular frequency. Because the structural–acoustic system is open-loop stable, the open-loop power flow should be less than or equal to zero for all frequencies. Inspection of Figure 12 shows this to be the case. The negative spikes in this transfer function occur at the structural resonances and indicate that power is being dissipated by the damping in the beam. Thus, the acoustics excite the beam at its natural frequencies and the beam dissipates energy by structural damping mechanisms. The roll-off in the open-loop power flow transfer function is due to the frequency shaping of the disturbance. The closed-loop power flow is much lower than for the open-loop, indicating good performance. The fact that the closed-loop power flow is negative for all frequencies indicates that power is being dissipated at all frequencies, indicating that the reverberant closed-loop system will be stable. A check of this fact using the fully coupled model shows that, indeed, it is stable.

In this example, the structural model used in the dereverberated control design model and the fully reverberant evaluation model are identical. In practice, however, this will seldom be the case, as the structural model will always have some error compared to the real system. LQG methods tend to be very sensitive to these errors, often resulting in closed-loop instability. Over the last decade, however, tremendous progress has been made in the field of $\mathcal{H}_2$ robust control for uncertain structural systems, see reference [12] for a survey of robust $\mathcal{H}_2$ control techniques. Because the power flow cost functional was cast as an $\mathcal{H}_2$ problem, all of these robust control design tools are available for use in the structural–acoustic power flow control problem.

In the present paper, the LQG power flow technique was derived using an acoustically dereverberated state-space model based on a structural finite element model. This state-space model uses structural degrees of freedom as the states of the model and the full mass, stiffness, and damping matrices in the formulation of the state transition (**A**) matrix. For realistic systems, which typically have many thousands of degrees of freedom, this physical control design model will be of too large an order to be useful. Fortunately, a much lower order formulation for this acoustically dereverberated design model is also possible [13], in which the full structural model is replaced with a modal representation and the full local acoustic model is replaced with a set of incoming and outgoing acoustic power flow "modeshapes". At present, the LQG power flow control design technique has only been formulated for the case where a structural finite element model is available or can be constructed. For most practical structures, this is not too great an assumption.

The only requirements for practical implementation of this power flow control methodology are a finite element model of the enclosing structure (or modal representation), a model of the coupling between the structure and the acoustic field at the structural boundary, and a description of the outgoing acoustic waves from the structure. The structural model, including the structural actuators and sensors, is the most readily available of these. Either the full physical model or a reduced modal model can be used for the structural model. The coupling model describes the influence of a unit pressure at the boundary on the displacements of the structure [11]. This coupling model can be thought of as a generalized area matrix because the pressure acts on the area of an element and in a manner similar to structural mass matrices can be lumped or consistent. The area for a given element is broken up into effective areas for the nodes that form the vertices of the element. For a lumped matrix, the effective areas for each element that includes a given node are summed up. In the consistent matrix, however, there is coupling between the pressure on a given node and the displacements at neighboring nodes. Note that pressure acts normal to the structural surface, so care must be exercised when determining the coupling matrix to account for this fact. The outgoing acoustic waves are described by equation (44) for each of the nodes at the structural–acoustic boundary. With the description of the outgoing waves, the procedure in equations (46)–(50) can be applied. Typically, however, there will be many thousands of nodes at the structural–acoustic boundary, making the book keeping task for the incoming and outgoing acoustic waves daunting. A way to alleviate this book keeping task is to use a set of incoming and outgoing acoustic wave "modeshapes" in a manner similar to that for the structural modal model. Care must be exercised, however, that the chosen "modeshapes" span the incoming/outgoing waveforms that would typically be encountered. A good set of "modeshapes" to use is the lowest several rigid-walled acoustic eigenvectors evaluated at the structural–acoustic boundary. The last step is to include in the local model any acoustic sensors at the structure–acoustic boundary that will be used for feedback, which is performed using equation (45). Once this is done, the power flow control law is determined using the LQG (possibly robustified) design technique.

As mentioned previously, this structural model will be in error to some degree. An alternative to the analytical model is a model determined from system identification methods, which are typically much more accurate than the analytical methods. At present, though, formulations of the LQG power flow technique using identified models have not been constructed. One problem with identified models is that the identified models only capture behavior that can be physically measured. The power flow formulation, however, requires performance outputs and disturbance inputs that are not physical, such as the incoming and outgoing pressure wave amplitudes. Future research, therefore, will be directed toward obtaining LQG power flow formulations that have relaxed measurement requirements so that identified models may be used.

6. CONCLUSIONS

The primary method for deriving an impedance matching compensator involves minimizing the power flow at the structure–acoustic boundary. This solution method is quite complicated even for very simple problems, making its application to realistic systems impractical if not impossible. Fortunately, the power flow minimization can be recast in terms of an LQG problem using a structural model with only local acoustic coupling. The LQG method has been shown to be equivalent to the power flow method for a simple structural–acoustic sample problem. In the LQG framework, realistic problems can be handled with ease. This has been demonstrated for a relatively simple two-dimensional sample problem that captures all the essential features of the realistic acoustic launch load alleviation problem.

ACKNOWLEDGMENTS

The authors would like to acknowledge the Air Force Office of Scientific Research for support of this research under AFOSR Grant No. F49620-96-1-0290. An additional acknowledgment goes to Captain Jeanne Sullivan and Steve Griffin of the Air Force Research Laboratory, and Paul Janzen of the McDonnell Douglas Company for their assistance in the pursuit of this research.

REFERENCES

1. B. Houston, M. Marcus, J. Bucaro and E. Williams 1996 *Proceedings of the Second AIAA/CEAS Aeroacoustics Conference*, *AIAA Paper* 96-1723. Active control of payload fairing interior noise using physics-based control laws.
2. S. Vadali and A. Das 1996 *AIAA Guidance*, *Navigation and Control Conference*, *AIAA Paper* 96-3756. Active control of structural–acoustic systems: noise reduction in payload fairings.
3. V. V. Varadan, J. Kim and V. K. Varadan 1995 *Proceedings*, *Spie*, **2442**, 470–475. Optimal design of enclosures for active noise control and isolation.
4. D. W. Miller and A. H. von Flotow 1989 *Journal of Sound and Vibration* **128**, 145–162. A travelling wave approach to power flow in structural networks.

5. D. W. MILLER, S. R. HALL and A. H. VON FLOTOW 1990 *Journal of Sound and Vibration* **140**, 475–497. Optimal control of power flow at structural junctions.
6. D. G. MACMARTIN, D. W. MILLER and S. R. HALL 1991 in *Recent Advances in Active Control of Sound and Vibration*, 604–617. Structural control using active broadband impedance matching.
7. D. GUICKING and K. KARCHER 1984 *AIAA Journal of Vibration, Acoustics, Stress and Reliability in Design* **106**, 393–396. Active impedance control for one-dimensional sound.
8. R. M. GLAESE, D. W. MILLER and K. ASARI 1997 *Proceedings of the AIAA/ASME/AHS Adaptive Structures Forum, Kissimmee, FL*. A comparison of control design models for a one-dimensional structural–acoustic sample problem.
9. F. FAHY 1985 *Sound and Structural Vibration*. New York, NY: Academic Press.
10. D. G. MACMARTIN and S. R. HALL 1991 *AIAA Journal of Guidance, Control and Dynamics* **14**, 521–530. Control of uncertain structures using an $\mathcal{H}_\infty$ power flow approach.
11. M. PETYT 1985 in *Theoretical Acoustics and Numerical Techniques* (Filippi, P., editor), 51–103. Wien, Austria: Springer-Verlag. Finite element techniques for acoustics.
12. S. C. GROCOTT 1994 *Master's thesis, Massachusetts Institute of Technology*. Comparison of control techniques for robust performance on uncertain structural systems.
13. R. M. GLAESE 1997 *Ph.D. thesis, Massachusetts Institute of Technology, Cambridge, MA*. Impedance matching for structural–acoustic control.

APPENDIX: NOMENCLATURE

$(\cdot)^{\mathrm{H}}$	complex conjugate transpose
c_0, ρ_0	speed of sound and ambient density of acoustic medium
f, $\bar{f}$	structural force, forcing vector
i	imaginary number ($\sqrt{-1}$)
$\hat{k}$	acoustic wave number
m, k, c	scalar mass, spring, and damper values
s	Laplace variable
u, $\dot{u}$, $\ddot{u}$	structural displacement, velocity, acceleration
w_i, w_o	incoming and outgoing propagating wave amplitudes
y, z	state space sensor measurements, performance variables
A	cross-sectional area
A, **B**, **C**, **D**	state space matrices
$\mathbf{A}_{fs}$	fluid–structure coupling matrix
$E(\cdot)$	expected value operator
G, **H**	LQG regulator and estimator gains
$G(s)$	compensator transfer function
I	identity matrix
J	scalar cost function
$\mathbf{M}_s$, $\mathbf{K}_s$, $\mathbf{C}_{ds}$	structural mass, stiffness, and damping matrices
Q	linear quadratic regulator state weighting matrix
P	acoustic pressure
P_l, P_r	leftward and rightward propagating acoustic wave amplitudes

P_i, P_o	incoming and outgoing propagating acoustic wave amplitudes
$\mathcal{P}$	average power flow
$\mathcal{P}_m$	structure–acoustic boundary power matrix
η, ξ	sensor noise, process noise
ρ	penalty on control effort
ω	frequency